











Field-resolved space–time characterization of few-cycle structured light pulses: supplement

YANGYANG LIU,^{1,2}  SHIMA GHOLAM-MIRZAEI,³  DIPENDRA KHATRI,²  TRAN-CHAU TRUONG,²  TROIE D. JOURNIGAN,²  CHRISTIAN CABELLO,²  CHRISTOPHER LANTIGUA,²  ANDRÉ STAUDTE,³  PAUL B. CORKUM,³  AND MICHAEL CHINI^{2,4,*} 

¹*School of Optical and Electronic Information, Huazhong University of Science and Technology, Wuhan 430074, China*

²*Department of Physics, University of Central Florida, Orlando, Florida 32816, USA*

³*Joint Attosecond Science Laboratory, University of Ottawa and National Research Council Canada, 25 Templeton Street, Ottawa, Ontario K1N 6N5, Canada*

⁴*CREOL—The College of Optics and Photonics, University of Central Florida, Orlando, Florida 32816, USA*

**Michael.Chini@ucf.edu*

This supplement published with Optica Publishing Group on 13 June 2024 by The Authors under the terms of the [Creative Commons Attribution 4.0 License](https://creativecommons.org/licenses/by/4.0/) in the format provided by the authors and unedited. Further distribution of this work must maintain attribution to the author(s) and the published article's title, journal citation, and DOI.

Supplement DOI: <https://doi.org/10.6084/m9.figshare.25917157>

Parent Article DOI: <https://doi.org/10.1364/OPTICA.521764>

Field-Resolved Space-Time Characterization of Few-Cycle Structured Light Pulses: Supplement

YANGYANG LIU^{1,2}, SHIMA GHOLAM-MIRZAEI³, DIPENDRA KHATRI², TRAN-CHAU TRUONG², TROIE D. JOURNIGAN², CHRISTIAN CABELLO², CHRISTOPHER LANTIGUA², ANDRÉ STAUDTE³, PAUL B. CORKUM³ AND MICHAEL CHINI^{2,4,*}

¹*School of Optical and Electronic Information, Huazhong University of Science and Technology, Wuhan, 430074, China*

²*Department of Physics, University of Central Florida, Orlando FL 32816, USA*

³*Joint Attosecond Science Laboratory, University of Ottawa and National Research Council Canada, 25 Templeton Street, Ottawa, ON K1N 6N5, Canada*

⁴*CREOL – the College of Optics and Photonics, University of Central Florida, Orlando FL 32816, USA*

**Corresponding author: Michael.Chini@ucf.edu*

Supplementary Notes

Supplementary Note 1: Nonlinear compression of the mid-IR pulse

The experiments were carried out using mid-IR pulses produced by a two-stage optical parametric amplifier (OPA, Light Conversion ORPHEUS-ONE) pumped by a commercial Yb:KGW amplifier (KGW, potassium gadolinium tungstate; Light Conversion Carbide). The OPA idler is tunable from 2.2 to 4.5 μm , and provided 10 μJ , 90-fs pulses centered at a wavelength of 3.28 μm at a repetition rate of 10 kHz for these experiments. Both the multi- and few-cycle structured light are used to investigate the potential of the 3d TIPTOE technique. To obtain the few-cycle pulses, we temporally compressed the mid-IR OPA output to a duration of below 3 optical cycles by focusing the mid-IR pulse through three windows (2-mm-thick silicon, 5-mm-thick YAG and 2-mm-thick silicon). The pulse compression details are described clearly in our previous work [1].

Supplementary Note 2: Generation and characterization of the few-cycle Bessel-Gaussian beam

A schematic of the experimental setup for the generation and characterization of the Bessel-Gaussian beam using 3D TIPTOE is illustrated in Supplementary Fig. 1. After transmission and reflection, respectively, by a CaF_2 wedge pair, the few-cycle mid-IR pulse is split into an intense fundamental and weak perturbation pulse. The fundamental beam is a well-collimated near-Gaussian beam with $1/e^2$ diameter of 3 mm. The perturbation beam is converted into a Bessel-Gaussian beam, which is achieved by placing a narrow annular beam in the focal plane of a lens [2]. After reflection by a hole-drilled mirror and transmission through an adjustable iris aperture placed close to the hole-drilled mirror, the narrow annular beam is generated. After passing through a CaF_2 lens ($f=200$ mm) installed 200 mm away from the iris, the annular beam is converted into the Bessel-Gaussian beam. By using a second wedge pair, the perturbation Bessel-Gaussian beam and the fundamental beam are directed collinearly onto a silicon-based image sensor. The intensity of the Bessel-Gaussian beam is around 0.1% that of the fundamental beam. By scanning the delay using a piezo stage installed in the perturbation arm, the modulated photocurrent signal in each pixel of the image sensor can be measured. In TIPTOE, the modulation amplitude is directly proportional to the electric field of the perturbation pulse, and therefore provides a direct measurement of the laser waveform. By taking the Fourier Transform of the waveform, the spatial phase of the Bessel-Gaussian beam can be retrieved, as shown in Supplementary Fig. 3. The spatial phase in the center spot or the n^{th} ring remains constant, while there is an evident π phase shift in the adjacent rings. This is in good agreement with the known properties of Bessel-Gaussian beam, and confirms the good capability of the 3D TIPTOE technique in characterizing the spatial and temporal properties of the structured light.

Supplementary Note 3: Generation and characterization of the RPVB

The experimental setup for the generation and characterization of the RPVB is schematically illustrated in Supplementary Fig. 2. The input pulse is first split into an intense fundamental and weak perturbation pulse by a CaF_2 wedge pair. The perturbation beam is converted into the RPVB by using a segmented half wave plate and $f=200$ mm CaF_2 lens. The segmented HWP comprises of four small HWPs. The distance between the adjacent HWPs is 0.1 mm, and the fast axis of each HWP is perpendicular to that of the adjacent HWP. Finally, the perturbation RPVB and the fundamental beam are combined using a second wedge pair and directed collinearly onto the silicon-based image sensor. A schematic diagram of the segmented HWP is shown in the inset of the Supplementary Fig. 1.

Fully characterizing the RPVB requires the measurement of the polarization state. As the RPVB is expected to be fully polarized, the polarization state is described using Jones vectors. Briefly, the polarization state can be identified when the amplitude and phase of the P- and S-polarized pulses are measured. To do so requires installation of a HWP in the fundamental arm to control the polarization state of the fundamental pulse, allowing consecutive measurements of the TIPTOE modulation with S- and P-polarized fundamental pulses while maintaining interferometric stability. The interferometric stability is obtained by co-propagating a 532 nm CW pilot beam in the 3D TIPTOE interferometer, and simultaneously recording the TIPTOE signal and the interference fringes of the recombined pilot beam.

Supplementary Note 4: Carrier-envelope phase influence on characterizing pulses using 3D TIPTOE

While the TIPTOE technique can be used to characterize the full electric field waveform, including the carrier-envelope phase (CEP) [1, 3], TIPTOE measurements can also be performed with a CEP-unstable source [4-6]. This is because the absolute phase of the measured TIPTOE modulation is not the CEP of the perturbation pulse, but instead reflects the carrier-envelope phase difference between the fundamental and the perturbing pulses. Therefore, the TIPTOE modulation reflects the perturbing pulse CEP only when the fundamental pulse CEP is locked to zero. In our 3D TIPTOE experiments, the CEP of the mid-infrared source is expected to be stable, but is not set to zero. However, this does not impact the measurement of the spatial phase, as the extracted waveform is accurate up to a constant global phase.

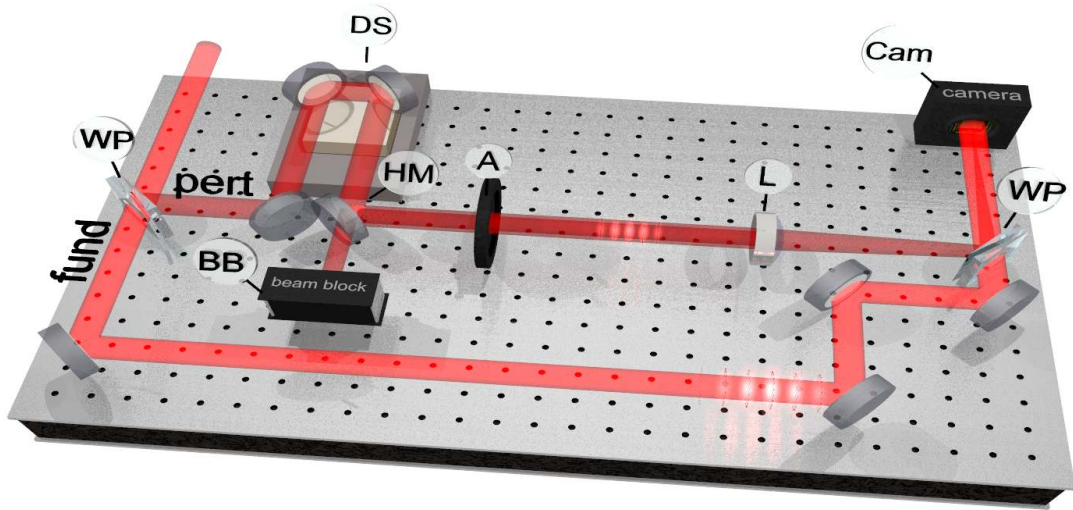


Fig. S1. Experimental setup for the generation and characterization of the Bessel-Gaussian beam using 3D TIPTOE. WP: CaF₂ wedge pair; fund: fundamental pulse; pert: perturbing pulse; DS: delay stage; HM: hole-drilled mirror; BB: beam block; A: circular aperture; L: lens; Cam: camera. CaF₂ wedges with a wedge angle of 2.8 degrees and the minimum thickness of 0.5 mm are used throughout this paper. The input laser is s-polarized (vertical polarization) and the incidence angle for both wedge pairs is 45 degrees.

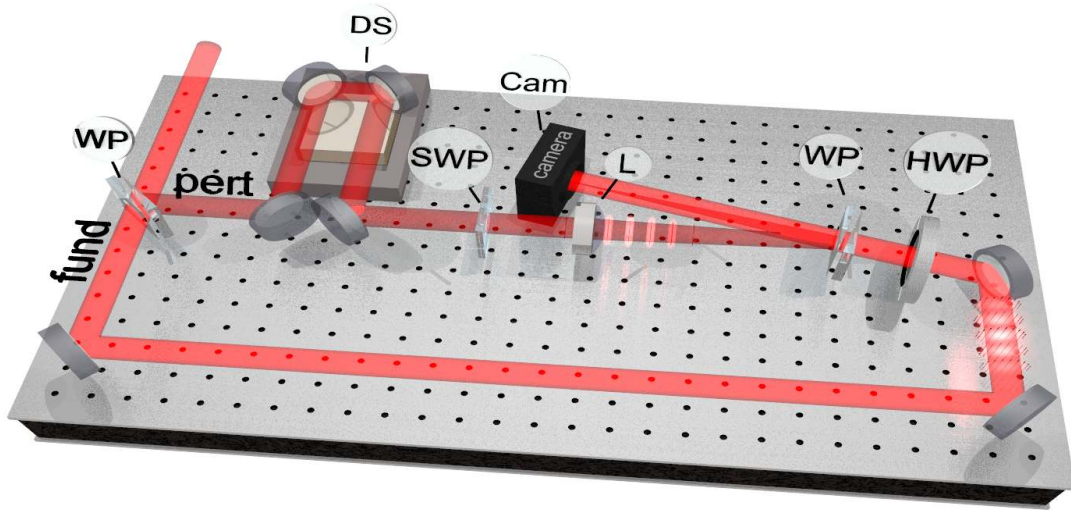


Fig. S2. Experimental setup for the generation and characterization of the radially polarized vector beam (RPVB) using 3D TIPTOE. WP: wedge pair; fund: fundamental pulse; pert: perturbing pulse; DS: delay stage; SWP: segmented zero-order half-wave plate; L: focusing lens; HWP: half-wave plate; Cam: camera. The input laser is s-polarized (vertical polarization), and the incidence angle for the first wedge pair is 45 degrees. 3D TIPTOE delay scans are performed for both s- and p-polarized fundamental pulses, in order to sample both polarization components of the RPVB, by rotating the HWP. For the second wedge pair, the incidence angle is kept below 5 degrees, to ensure equal reflectivity for s- and p-polarized components of the RPVB.

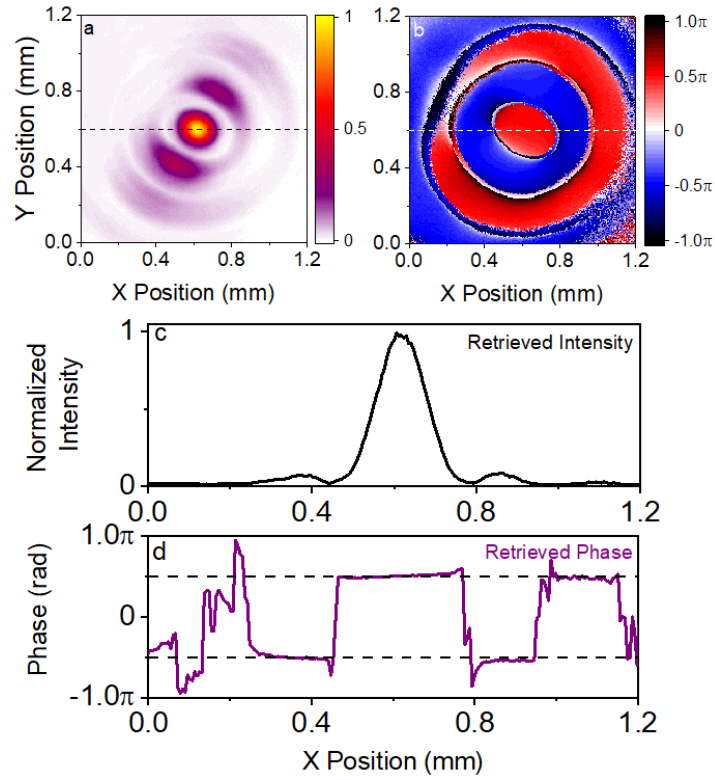


Fig. S3. The 3D TIPTOE-retrieved spatial phase distribution of the Bessel-Gaussian beam. **a** The intensity profile of the Bessel-Gaussian beam retrieved by the 3d TIPTOE, **b** the 3d TIPTOE retrieved spatial phase distribution of the Bessel-Gaussian beam, **c** the reconstructed intensity distribution of the horizontal line passing through the center of the Bessel-Gaussian beam, and **d** the relative value of the spatial phase along the horizontal line. There is an evident π phase shift between the adjacent rings. The two dashed lines in panel d are added for eye-guidance to show the π phase difference.

Supplementary Reference

1. Y. Liu, J. E. Beetar, J. Nesper, *et al.*, “Single-shot measurement of few-cycle optical waveforms on a chip,” *Nat. Photon.* **16**, 109-112 (2022).
2. J. Durnin, J. J. Miceli & J. H. Eberly, “Diffraction-free beams,” *Phys. Rev. Lett.* **58**, 1499–1501 (1987).
3. S. B. Park, K. Kim, W. Cho, *et al.*, “Direct sampling of a light wave in air,” *Optica* **5**, 402–408 (2018).
4. W. Cho, S. I. Hwang, C. H. Nam, *et al.*, “Temporal characterization of femtosecond laser pulses using tunneling ionization in the UV, visible, and mid-IR ranges,” *Sci. Rep.* **9**, 16067 (2019).
5. Y. Liu, S. Gholam-Mirzaei, J. E. Beetar, *et al.*, “All-optical sampling of few-cycle infrared pulses using tunneling in a solid,” *Photon. Res.* **9**, 929–936 (2021).
6. J. Blöchl, J. Schötz, A. Maliakkal, *et al.*, “Spatiotemporal sampling of near-petahertz vortex fields,” *Optica* **9**, 755-761 (2022).